

Absolute Reactive Cross Section for H Atom Formation in the Reaction of Translationally Energetic O(¹D) Atoms with Methane

Richard A. Brownsword, Matthias Hillenkamp, Patricia Schmiechen, and Hans-Robert Volpp*

Physikalisch-Chemisches Institut der Universität Heidelberg, Im Neuenheimer Feld 253, D-69120 Heidelberg, Germany

Hari P. Upadhyaya

Chemistry Division, Bhabha Atomic Research Centre, Bombay 400 085, India

Received: January 6, 1998; In Final Form: February 26, 1998

The dynamics of the H atom formation channel in the reaction of metastable oxygen atoms O(¹D) with methane were studied in the gas phase using the pulsed laser photolysis/vacuum-UV laser-induced fluorescence “pump-and-probe” technique. Translationally energetic O(¹D) atoms with an average collision energy of 37 kJ/mol in the O(¹D)–CH₄ center-of-mass system were generated by laser photolysis of N₂O at 193 nm. Nascent H atoms produced in reactive collisions of O(¹D) with room-temperature CH₄ molecules were detected with sub-Doppler resolution via (2p²P ← 1s²S) laser-induced fluorescence. An absolute reaction cross section of σ^H(37 kJ/mol) = 1.4 ± 0.5 Å² was determined for the H atom formation channel by means of a calibration method. From the H atom Doppler profiles measured under single-collision conditions the product translational energy release was determined.

I. Introduction

Reactions of electronically excited atoms are of great practical importance in a variety of media, for example, electrical discharges and planetary atmospheres.^{1,2} On the more fundamental side, the physical or chemical transformation of atomic electronic energy into product translational, vibrational, rotational, and/or electronic energy can provide important information for testing dynamical models of molecular interactions in the gas phase.³

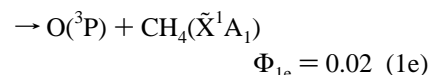
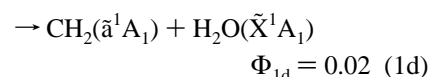
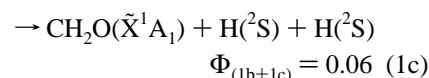
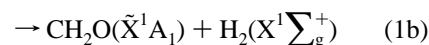
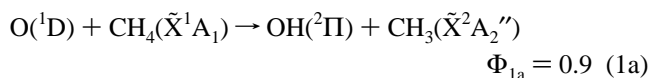
Stratospheric reactions of metastable oxygen atoms O(¹D) with small hydride molecules⁴—most of them leading to OH radicals—partly determine the chemistry of the earth’s ozone layer via the HO_x cycle.⁵ Besides the O(¹D) + H₂O(¹X¹A₁) → OH(²Π) + OH(²Π) reaction, the reaction O(¹D) + CH₄(¹X¹A₁) is an important source of OH radicals in the stratosphere.^{2b} The high reactivity of the latter one has been attributed to the possibility for the two singlet reagents to correlate with the singlet ground state (¹X¹A) of the CH₃OH[‡] reaction intermediate which can be formed via insertion of O(¹D) into the C–H bond:⁶



The unimolecular decomposition of CH₃OH(¹X¹A), which plays an important role in combustion chemistry,⁷ has been studied both theoretically⁸ and experimentally behind incident shock waves in the temperature range 1400–2200 K and after infrared multiple photon^{10a} and UV-laser photoexcitation at 193 nm.^{10b,c}

The overall rate for reaction 1 has been measured by different groups leading to a recommended value of $k_1 = 1.5 \times 10^{-10}$ cm³ molecule⁻¹ s⁻¹ for the room-temperature rate constant.¹¹ In addition, the rate constant was found to be temperature independent in the range 198 ≤ T/K ≤ 357.¹² Only recently

was the product channel distribution of (1) characterized in great detail in a room-temperature reaction kinetics study by Hack and Thiesemann,⁶ who reported the following values:



The above channel distribution is based on kinetic calibration measurements in which OH(²Π), CH₂O(¹X¹A₁), CH₂(¹ā¹A₁), and O(³P) reaction products were detected using the laser-induced fluorescence (LIF) method.

State-resolved reaction dynamics studies of channel (1a), in which OH and CH₃ radicals were detected, have been carried out by a number of groups.^{13,14} The observed nonstatistical rovibrational population distributions were ascribed to a fast dissociation of the CH₃OH[‡] reaction intermediate, on a time scale too short to allow for complete intramolecular relaxation. From classical chemical quenching experiments, a lifetime of 0.8 ps was deduced,¹⁵ while a more recent subpicosecond laser photolysis pump-and-probe measurement of the appearance of OH($\nu=0$) following the 267 nm photolysis of CH₄•O₃ van der Waals complexes yielded a value of about 3 ps.¹⁶ As pointed

* To whom correspondence should be addressed.

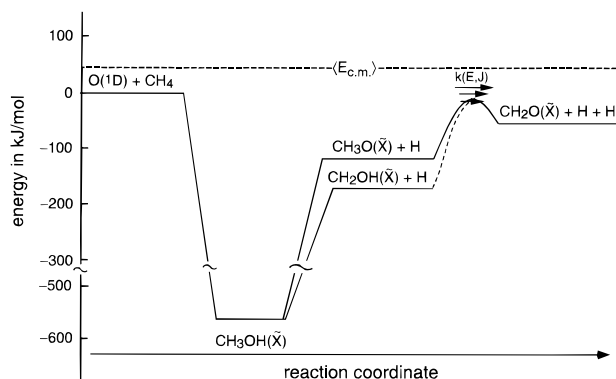
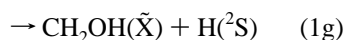


Figure 1. Schematic potential energy diagram for the different H atom formation channels in the $O(^1D) + CH_4$ reaction. $\langle E_{c.m.} \rangle$ denotes the experimental collision energy in the $O(^1D) - CH_4$ reagents' center-of-mass system. The consecutive three-body H atom formation pathway, as suggested in ref 6, is also included.

out in ref 17, the chemical quenching experiments of ref 15 did not determine whether the $O(^1D)$ atoms generated by 185 nm photolysis of N_2O were thermalized prior to reaction with CH_4 . Recently Olzmann¹⁸ used the statistical adiabatic channel model (SACM)¹⁹ to investigate the influence of different nascent angular momentum and internal energy distributions on the lifetime of CH_3OH^+ formed by $O(^1D) + CH_4$. His results suggest that the shorter lifetime observed in the chemical quenching experiments could be due to the incomplete translational relaxation of the initially translationally highly excited $O(^1D)$. Experiments in which velocity-aligned $O(^1D)$ atoms generated by polarized 193 nm laser photolysis of N_2O were employed indicate that at higher reagent collision energies, reaction 1a "lies closer to the direct limit".²⁰ This result was based on the analysis of Doppler profiles of $OH(v=0, N=19)$ and $OH(v=4, N=8)$.²⁰ More recently, indications for a long-lived reaction intermediate were found in an analysis of $OH(v=0, N=5)$ Doppler profiles.²¹

Compared to the number of dynamics studies of reaction 1a, rather little work has been done on the other possible channels. In a crossed molecular beam study, methoxy radicals (CH_3O) and/or hydroxymethyl radicals (CH_2OH) were suggested to be formed as primary products via²²



The mass signal of formaldehyde (CH_2O) observed in these studies was attributed to fragmentation of CH_3O and/or CH_2OH in the ionizer. In the same CMB study, no H_2 could be observed and it was estimated that $\Phi_{1b} < 0.25\Phi_{(1f+1g)}$. Figure 1 shows the potential energy diagram for the different H atom formation channels.

Gas-phase experiments in which H atom reaction products were directly observed were carried out by Bersohn and co-workers²³ and Kawasaki and co-workers,²⁴ which gave relative H atom yields of 0.24 and 0.14, respectively. In both studies the laser photolysis of O_3 at 248 nm was used to generate translationally energetic $O(^1D)$ atoms with an average collision energy of $\langle E_{c.m.} \rangle \approx 24$ kJ/mol. A significant difference in the values of the product energy release between the gas-phase^{23,24} and the molecular beam²² experiments was observed, and the discrepancy was attributed to the higher collision energy of about 27 kJ/mol as present in the molecular beam.

In the present study, the well-characterized 193 nm laser photolysis of $N_2O(^1\Sigma^+) \rightarrow O(^1D) + N_2(^1\Sigma_g^+)$ ^{25,26} was used to

generate translationally energetic $O(^1D)$ atoms with a well-defined average collision energy of $\langle E_{c.m.} \rangle = 37$ kJ/mol in order to investigate the suggested dependence of the product energy release on the collision energy. In addition, an absolute reaction cross section for H atom production was measured that allows for comparison with earlier studies of the $O(^1D) + CH_4$ reaction in which relative H atom product yields were estimated using the $O(^1D) + D_2 \rightarrow OD + D$ reaction as a reference.^{23,24}

II. Experimental Section

Laser photolysis/vacuum-UV laser-induced fluorescence (LP/VUV-LIF) "pump-and-probe" reaction dynamics studies and absolute H atom formation cross section measurements were carried out in a flow apparatus similar to the one used in our gas-phase reaction dynamics studies of the $O(^1D) + H_2/D_2/HD$ reactions.²⁷ The experimental technique has also been described in detail in ref 27; therefore, only a brief summary of the experimental method will be given in the following.

Mixtures of room temperature N_2O (99.999%) and CH_4 ($\geq 99.998\%$) were pumped through the flow reactor; both N_2O and CH_4 were used without further purification. The gas flows were regulated by calibrated flow meters. In the reaction dynamics studies the total pressure in the reaction cell was $p_{tot} = 100 - 130$ mTorr, measured by an MKS Baratron. The $[N_2O]:[CH_4]$ ratio was typically between 1:4 and 1:6. For the calibration measurements, HCl (99.999%) could be passed through the reactor at a pressure between 15 and 40 mTorr.

An ArF excimer laser ($\lambda_{pump} = 193$ nm) was used to generate energetic $O(^1D)$ reactants by pulsed photolysis of the N_2O precursor molecules. A cylindrical lens (1 m focal length) was used to partially focus the photolysis beam. Intensities were typically between 15 and 50 mJ/cm². The pump laser beam was determined to be essentially unpolarized, and it is therefore expected that any possible anisotropy of the photodissociation process would be largely averaged out. The duration of the pump laser pulse was about 15 ns. Typically 100–250 ns after the pump laser pulse, nascent H atoms produced in the reactive collisions with CH_4 molecules were detected by a probe laser pulse (duration $\approx 15 - 20$ ns) with sub-Doppler resolution via ($2p^2P \leftarrow 1s^2S$) VUV-LIF at the H atom Lyman- α wavelength (121.567 nm). The present experimental conditions allowed the measurement of the Doppler profiles of H atoms produced under single-collision conditions in the $O(^1D) + CH_4$ reaction.

The probe beam was carefully aligned to overlap the photolysis beam at right angle in the viewing region of the LIF detector. The quality of the spatial overlap of the pump and probe laser beams was checked in order to ensure that no H atoms produced in the reaction can escape the detection region during the pump/probe delay time of the experiment. This was done by recording H atom Doppler profiles in the 193 nm photolysis of HCl at different pump/probe delay times. HCl photolysis at 193 nm leads to very fast H atoms ($v_H \approx 19\,300$ m/s) and the invariance of the line shape, in particular in the region around the center of the profile (which originates from H atom with a velocity vector perpendicular to the probe laser propagation direction) is a very sensitive check for "fly-out". From the results of the HCl photolysis studies it can be ruled out that the measured reaction cross section we report is affected by "fly-out" of H atoms produced in the reaction.

Tunable narrow-band VUV-laser light was generated using the Wallenstein method in which resonant third-order sum-difference frequency conversion of pulsed dye laser radiation in a phase-matched Kr–Ar mixture²⁸ is employed. In the Kr mixing scheme used to generate the VUV radiation ($\omega_{VUV} =$

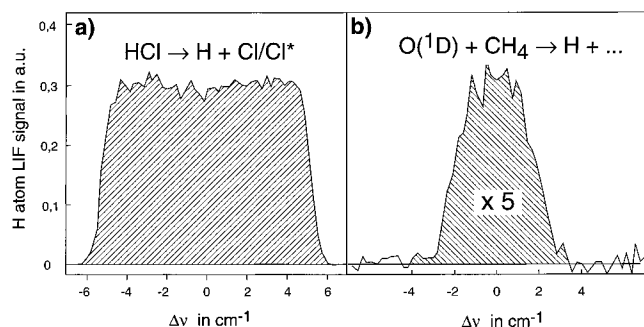


Figure 2. Comparison of the H atom reference signal (integrated area of the line profile) produced in the 193 nm photolysis of 21 mTorr of HCl with the H atom signal observed in the O(¹D) + CH₄ reaction 220 ns after pulsed laser photolysis of 21 mTorr of N₂O and 106 mTorr of CH₄. Details of the calibration method for the absolute reactive cross-section measurement are explained in the text. Centers of the LIF spectra correspond to the H atom Lyman- α transition ($\nu_0 = 82\,259\text{ cm}^{-1}$).

$2\omega_R - \omega_T$) the laser radiation of ω_R ($\lambda_R = 212.55\text{ nm}$) is resonant with the Kr 4p–5p ($1/2, 0$) two-photon transition and held fixed during the experiments, while ω_T is tuned from 844 to 846 nm to generate VUV laser radiation covering the H atom Lyman- α transition. The fundamental laser radiation was obtained from two dye lasers, simultaneously pumped by a XeCl excimer laser. In the first dye laser, Coumarin 120 was used to generate the 425.10 nm radiation which was subsequently frequency doubled in a BBO II crystal in order to obtain $\lambda_R = 212.55\text{ nm}$. $\lambda_T = 844\text{--}846\text{ nm}$ was obtained by operating the second dye laser with Styryl 9 dye.

Unconverted laser light was carefully separated from the generated Lyman- α radiation via a lens monochromator followed by a light baffle system. For the Lyman- α laser light a bandwidth of $\Delta\nu_{\text{Ly}\alpha} = 0.4\text{ cm}^{-1}$ was determined in separate experiments from H atom Doppler-profiles measured under thermalized conditions ($T_{\text{trans}} \approx 300\text{ K}$). The H atom LIF signal was measured through a band-pass filter ($\lambda_{\text{center}} = 122\text{ nm}$, fwhm = 20 nm) by a solar blind photomultiplier positioned at right angles to the VUV probe laser beam.

In ref 29 it was found that the VUV probe radiation itself can produce appreciable H atom LIF signals via CH₄ photolysis. To subtract these “background” H atoms from the H atoms produced in the reaction O(¹D) + CH₄, an electronically controlled mechanical shutter was inserted into the photolysis beam path. At each point of the H atom line scan, the signal was first measured with the shutter opened and again measured with the shutter closed. A point-by-point subtraction procedure was adopted, to obtain directly and on-line a signal free from any background H atoms produced by VUV probe laser initiated photochemistry.

The VUV probe beam intensity was monitored after passing through the reaction cell with an additional solar blind photomultiplier. The LIF signal, VUV probe beam intensity, and the photolysis laser intensity (monitored with a photodiode) were recorded with a boxcar system and transferred to a microcomputer where the LIF signal was normalized to both photolysis and VUV probe laser intensities. Because of the different degrees of absorption of the VUV probe laser radiation by the N₂O/CH₄ and HCl a correction had to be applied to ensure that the measured H atom LIF signal is normalized to the probe laser intensity as actually present in the detection region. In the absorption correction for the VUV probe laser intensity a value of $2.0 \times 10^{-17}\text{ cm}^2$ for the optical absorption cross sections of CH₄ at the Lyman- α wavelength was used.²⁹ Values of 2.6×10^{-18} and $1.4 \times 10^{-19}\text{ cm}^2$ for the Lyman- α optical

absorption cross sections of N₂O and HCl were determined in the present study.

Finally, to obtain a satisfactory S/N ratio, each point of the H atom Doppler profiles (Figure 2) was averaged over 30 laser shots. Measurements were carried out at a repetition rate of 6 Hz.

III. Results

A. Absolute Reaction Cross Section for H Atom Formation. The absolute reaction cross section σ^{H} for the H atom formation channel in the O(¹D) + CH₄ reaction was obtained by calibrating the H atom signal S_R measured in the reaction against the H atom signal S_{HCl} from well-defined H atom number densities generated by photolyzing HCl. S_R and S_{HCl} are defined by the integrated areas under the H atom fluorescence curves. The absolute reaction cross section was determined using the following expression derived in ref 27a:

$$\sigma^{\text{H}}(E_{\text{c.m.}}) = \{S_R \sigma_{\text{HCl}}[\text{HCl}]\} / \{S_{\text{HCl}} \sigma_{\text{N}_2\text{O}}[\text{CH}_4][\text{N}_2\text{O}]v_{\text{rel}}\Delta t\} \quad (2)$$

v_{rel} is the average relative velocity, $\langle E_{\text{c.m.}} \rangle = 1/2\mu v_{\text{rel}}^2$ stands for the corresponding average center-of-mass collision energy of the reactants and μ is the reduced mass of the O(¹D)–CH₄ collision pair. $\langle E_{\text{c.m.}} \rangle$, and hence v_{rel} , can be calculated from the photolysis laser wavelength, the N₂(¹ Σ_g^+) + O(¹D) dissociation energy of the N₂O molecule and the measured internal state distribution of the N₂(¹ Σ_g^+) fragment,^{25a} as described in detail in ref 27a. Δt is the time delay between pump and probe laser pulses determined by measuring the time difference between photolysis and probe scattered light pulses observed on a fast oscilloscope (Tektronik Model 485, 350 MHz). The number densities [HCl], [CH₄], and [N₂O] were directly calculated from the partial pressures. For the optical absorption cross sections of HCl and N₂O at the photolysis of 193 nm the following values from refs 30 and 31 were used: $\sigma_{\text{HCl}} = 8.1 \times 10^{-20}\text{ cm}^2$ and $\sigma_{\text{N}_2\text{O}} = 9.0 \times 10^{-20}\text{ cm}^2$. Both the 193 nm photodissociation of HCl and N₂O proceed with a quantum yield of unity for H and O(¹D) atom formation, respectively.¹¹

Figure 2 shows typical H atom Doppler profiles obtained in the O(¹D) + CH₄ reaction and in the 193 nm photodissociation of HCl. The evaluation of a series of 10 independent measurements, each consisting of three H atom profiles measured under reaction conditions and one profile obtained in the HCl photolysis, gave the following average value (quoted error represents 2 standard deviations) for the absolute reaction cross section for H atom formation in the O(¹D) + CH₄ reaction: $\sigma^{\text{H}}(37\text{ kJ/mol}) = 1.4 \pm 0.5\text{ \AA}^2$.

B. Average Product Translational Energy. From the H atom Doppler profiles the average kinetic energies, $E_{\text{t}}^{\text{LAB}}(\text{H})$, of the H atoms in the laboratory frame can be determined. Because the measured H atom Doppler profiles reflect, via the linear Doppler shift $\Delta\nu = \nu - \nu_0 = v_z\nu_0/c$, directly the distribution $f(v_z)$ of the velocity component v_z of the absorbing H atoms along the propagation direction of the probe laser beam, for an isotropic velocity distribution, $f(v_x) = f(v_y) = f(v_z)$, the average translational energy in the laboratory frame is given by $E_{\text{t}}^{\text{LAB}}(\text{H}) = 3/2m_{\text{H}}\langle v_z^2 \rangle_{\text{H}}$, where $\langle v_z^2 \rangle_{\text{H}}$ represents the second moment of the laboratory velocity distribution of the H atoms:

$$\langle v_z^2 \rangle_{\text{H}} = \int_{-\infty}^{\infty} v_z^2 f(v_z) dv_z = c^2 \int_{-\infty}^{\infty} [(v - \nu_0)/\nu_0]^2 g(v) dv \quad (3)$$

c is the speed of light and $g(v)$ is the normalized H atom Doppler profile. $g(v)$ was obtained directly by fitting an empirical

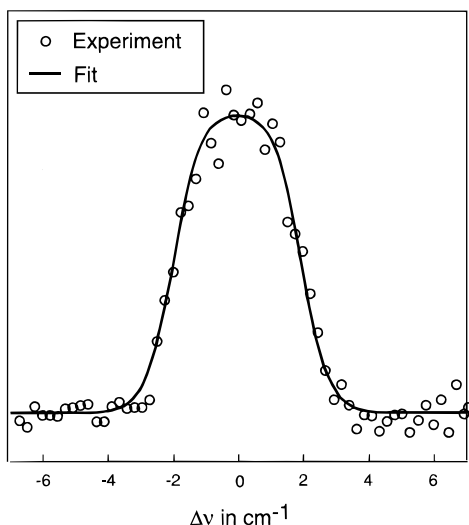


Figure 3. Doppler profile of H atoms produced in the O(¹D) + CH₄ reaction. Solid line represents the normalized Doppler line shape $g(\nu)$ obtained as a result of a fit using a symmetric double-sigmoidal function.

function to the measured H atom fluorescence data as depicted in Figure 3. For that purpose the very flexible symmetric double sigmoidal function³² was chosen because the measured H atom profiles could be better described by that functional form than by a Gaussian one. The latter one would imply a Maxwell–Boltzmann translational energy distribution. In principle, it should be taken into consideration that the measured spectral profile represents a convolution of the Doppler profile of the absorbing H atom and the probe laser spectral profile. However, in the present study the VUV probe laser bandwidth (0.4 cm⁻¹) was so small compared to the width of the line profile due to the Doppler broadening (fwhm \approx 4 cm⁻¹) that no back-correction due to the finite probe laser bandwidth was necessary.

The complete set of 30 measured H atom Doppler profiles was evaluated to determine a value of $E_t^{\text{LAB}}(\text{H}) = 38.2 \pm 9.1$ kJ/mol. The average energy released into product translation in the CM frame, $\langle E'_t \rangle$, was determined using the following expression:^{27b,33}

$$\langle E'_t \rangle = \frac{m_{\text{CH}_3\text{OH}}}{m_{\text{CH}_3\text{O}}} \left(E_t^{\text{LAB}}(\text{H}) - \langle E_t^{\text{LAB}}(\text{CH}_3\text{OH}) \rangle \frac{m_{\text{H}}}{m_{\text{CH}_3\text{OH}}} \right) \quad (4)$$

where $E_t^{\text{LAB}}(\text{CH}_3\text{OH})$ is the average kinetic energy of the center-of-mass motion in the laboratory frame, which can be calculated via

$$\langle E_t^{\text{LAB}}(\text{CH}_3\text{OH}) \rangle = \langle E_t^{\text{LAB}}(\text{O}(^1\text{D})) \rangle \frac{m_{\text{O}}}{m_{\text{CH}_3\text{OH}}} + \langle E_t^{\text{LAB}}(\text{CH}_4) \rangle \frac{m_{\text{CH}_4}}{m_{\text{CH}_3\text{OH}}} \quad (5)$$

Using eqs 4 and 5, a value of $\langle E'_t \rangle = 36.8 \pm 8.8$ kJ/mol was obtained. From this $f'_t = \langle E'_t \rangle / E_{\text{avl}}$, the fraction of the available energy released to product translation, can be determined. E_{avl} is given by $\langle E_{\text{c.m.}} \rangle - \Delta H_{\text{R}}(298 \text{ K})$. The reaction enthalpies, $\Delta H_{\text{R}}(298 \text{ K})$, for the different energetically possible H atom producing reaction channels depicted in Figure 1 were calculated from the standard enthalpies of formation listed in Table 1. f'_t values obtained in the present study are listed in Table 2 together with the results of earlier studies at lower collision energies.^{22–24}

IV. Discussion

A. Absolute Reactive Section and Product Yield for H Atom Formation. The value $\sigma^{\text{H}}(37 \text{ kJ/mol}) = 1.4 \pm 0.5 \text{ \AA}^2$ obtained in the present study represents to the best of our knowledge the first absolute reaction cross section measured for the H atom formation channel of the O(¹D) + CH₄ reaction. Theoretical reaction cross sections are not available so far for a direct comparison although a potential energy surface (PES) has been calculated recently for the O(¹D) + CH₄ reaction, which includes the CH₃ + OH as well as the CH₃O + H reaction channel.³⁵ However, comparison is possible with H atom product yields obtained in nonequilibrium kinetics studies at $\langle E_{\text{c.m.}} \rangle = 24 \text{ kJ/mol}$ ^{23,24} and in a room-temperature kinetics measurement.²⁴

The H atom formation cross section measured in the present work at $\langle E_{\text{c.m.}} \rangle = 37 \text{ kJ/mol}$ corresponds to a H atom product yield of $\phi^{\text{H}} = \sigma^{\text{H}}(37 \text{ kJ/mol}) / \sigma^{\text{capt}}(37 \text{ kJ/mol}) = 0.30 \pm 0.11$. The capture cross section of $\sigma^{\text{capt}}(37 \text{ kJ/mol}) = 4.6 \text{ \AA}^2$ was calculated on the basis of a simple $\sigma^{\text{capt}}(E_{\text{c.m.}}) \propto E_{\text{c.m.}}^{-1/2}$ Langevin model^{3a} from the room-temperature capture cross section $\sigma^{\text{capt}}(300 \text{ K}) = 15.7 \text{ \AA}^2$ given in ref 18. The use of the Langevin model is consistent with the temperature independent thermal rate coefficient observed experimentally.¹² In Table 2, the present ϕ^{H} value is listed together with the H atom product yields of refs 23 and 24. H atom product yields at $\langle E_{\text{c.m.}} \rangle = 24 \text{ kJ/mol}$ were obtained by measuring the [H]/[D] product ratio in the reaction of translationally energetic O(¹D) atoms—generated by 248 nm O₃ photolysis—with a 1:1 mixture of CH₄ and D₂. To allow for a direct comparison between the results of refs 23 and 24, the ϕ^{H} value of 0.18 ± 0.03 listed in Table 2 was calculated from the [H]/[D] product ratio reported in ref 23 using the same O(¹D) + CH₄/D₂ rates as used in ref 24 for the evaluation of the nonequilibrium data.

The room temperature value $\phi^{\text{H}} = 0.13 \pm 0.01$ listed in Table 2 was determined from a similar [H]/[D] product ratio measurement carried out under experimental conditions where the O(¹D) atoms were expected to be thermalized by collisions with Ar buffer gas.²⁴ For comparison, another room-temperature value $\phi^{\text{H}} = 0.16 \pm 0.05$ is also included, which one obtains when the same [H]/[D] product ratio is evaluated using the recommended O(¹D) + CH₄ room-temperature rate constant of $(1.4 \pm 0.2) \times 10^{-10} \text{ cm}^3 \text{ s}^{-1}$ instead of the value $(2.2 \pm 0.2) \times 10^{-10} \text{ cm}^3 \text{ s}^{-1}$ used in the ϕ^{H} determination in ref 24.

Although the experimental uncertainties are considerable, comparison of the available ϕ^{H} values obtained at different collision energies suggest that the relative importance of H atom production in the O(¹D) + CH₄ reaction increases slightly with increasing reagent translational excitation.

B. Kinetic Energy Release. In Figure 4, the experimental product translational energy distribution is depicted together with statistical “prior” translational energy distributions for the different energetically possible H atom forming reaction channels. The “prior” distribution for the three-body product channel 1c was calculated using the “canonical” statistical model of Baer et al.³⁶ “Prior” distributions for the two-body fragmentation channels 1f and 1g were calculated using the formulas given in ref 37. The corresponding f'_t values are listed in Table 2. The product translational energy release determined in the present study at $\langle E_{\text{c.m.}} \rangle = 37 \text{ kJ/mol}$ is similar to the results of the gas-phase experiments of refs 23 and 24 carried out at a collision energy of $\langle E_{\text{c.m.}} \rangle = 24 \text{ kJ/mol}$. This indicates that the product translational energy release does not depend on the initial reagent translational excitation. The product translational energy estimated in the molecular beam study²² at an intermediate collision

TABLE 1: Standard Enthalpies of Formation $\Delta H_f^\circ(298\text{ K})$ and Reaction Enthalpies $\Delta H_R(298\text{ K})$ of Energetically Possible H Atom Product Channels in kJ/mol (Ref 11)^c

species	$\Delta H_f^\circ(298\text{ K})$	reaction channel	$\Delta H_R(298\text{ K})$	E_{avl}
$\text{CH}_4(\tilde{\text{X}})$	-74.81	$\text{O}(^1\text{D}) + \text{CH}_4 \rightarrow \text{CH}_3\text{O} + \text{H}$	-121	158 ^b
$\text{CH}_3\text{O}(\tilde{\text{X}})$	25 ^a	$\text{O}(^1\text{D}) + \text{CH}_4 \rightarrow \text{CH}_2\text{OH} + \text{H}$	-155	192 ^b
$\text{CH}_2\text{OH}(\tilde{\text{X}})$	-9 ^a	$\text{O}(^1\text{D}) + \text{CH}_4 \rightarrow \text{CH}_2\text{O} + \text{H} + \text{H}$	-37	74 ^b
$\text{CH}_2\text{O}(\tilde{\text{X}})$	-108.6			
$\text{O}(^1\text{D})$	438.9			
H	217.997			

^a Values recommended in ref 34. ^b Calculated for an average collision energy of $\langle E_{\text{c.m.}} \rangle = 37\text{ kJ/mol}$. ^c The available energy to the products is given by $E_{\text{avl}} = \langle E_{\text{c.m.}} \rangle - \Delta H_R(298\text{ K})$.

TABLE 2: H Atom Product Yield ϕ^{H} and Product Translational Energy Release f'_t in the $\text{O}(^1\text{D}) + \text{CH}_4$ Reaction

$\langle E_{\text{c.m.}} \rangle / T$	ϕ^{H}	$f'_{t(\text{CH}_3\text{O}+\text{H})}$ ^a	$f'_{t(\text{CH}_2\text{OH}+\text{H})}$ ^a	$f'_{t(\text{CH}_2\text{O}+\text{H}+\text{H})}$ ^a
37 kJ/mol	0.30 ± 0.11	0.23 ± 0.06	0.19 ± 0.05	0.50 ± 0.13
27 kJ/mol		0.42^b	0.35^b	0.99^b
24 kJ/mol	0.18 ± 0.03^c	0.25 ± 0.04^b	0.20 ± 0.03^b	0.60 ± 0.09^b
24 kJ/mol	0.14 ± 0.02^d	0.22 ± 0.01^b	0.18 ± 0.01^b	0.53 ± 0.03^b
300 K	0.13 ± 0.01^d			
300 K	0.16 ± 0.05^e			
300 K	0.12^f			

^a Values for $f'_t = \langle E'_t \rangle / E_{\text{avl}}$ were calculated using the reaction enthalpies listed in Table 1. The statistical “prior” expectation value for the two-body fragmentation channels is $f'_{t(\text{prior})} = 1/8$, the statistical “prior” expectation value for the three-body fragmentation channel is $f'_{t(\text{prior})} = 0.14$.

^b Calculated from the $\langle E'_t \rangle$ values given in refs 22–24. ^c Calculated from the $[\text{H}]/[\text{D}]$ ratio reported in ref 23 via formula 8 of ref 24 using the $\text{O}(^1\text{D}) + \text{CH}_4/\text{D}_2$ rates measured in ref 24. ^d Reference 24. ^e Calculated from the $[\text{H}]/[\text{D}]$ ratio reported in ref 24 using the $\text{O}(^1\text{D}) + \text{CH}_4$ room-temperature rate recommended in ref 11. ^f Calculated from the CH_2O yield reported in ref 6, assuming that CH_2O is produced in combination with two H atoms.

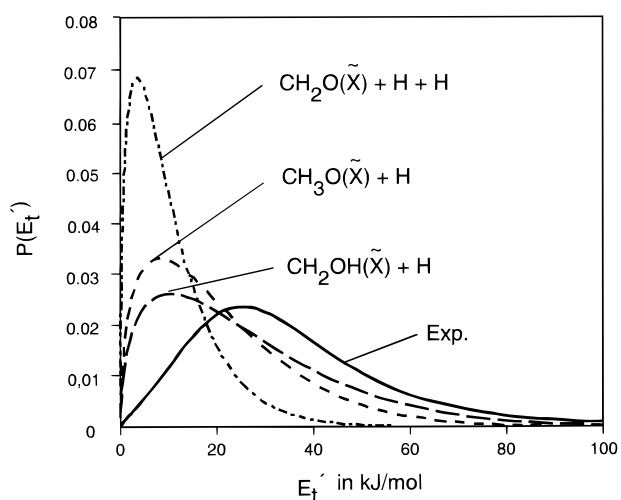


Figure 4. Comparison of the experimental product translational energy distribution (solid line) with statistical “prior” translational energy distributions calculated for different H atom forming reaction channels of the $\text{O}(^1\text{D}) + \text{CH}_4$ reaction (see text).

energy of $\langle E_{\text{c.m.}} \rangle = 27\text{ kJ/mol}$ suggests, however, a markedly higher value for the product translational energy release (see Table 2). Although the present study cannot finally resolve the discrepancy between the earlier gas-phase^{23,24} and beam results,²² it seems to be rather unlikely that the difference in the f'_t values is due to the difference in the $\text{O}(^1\text{D}) + \text{CH}_4$ collision energy.

The f'_t values observed in the gas-phase dynamics studies are significantly higher than the corresponding statistical “prior” expectation values (see Table 2). The observed nonstatistical energy partitioning would be consistent with a reaction mechanism in which the $\text{O}(^1\text{D})$ atom inserts into a C–H bond of the methane molecule leading to an energized $\text{CH}_3\text{OH}(\tilde{\text{X}})$ reaction complex, which dissociates prior to complete energy randomization. Based on experiments in which the H atom formation dynamics of the $\text{O}(^1\text{D}) + \text{CH}_4/\text{C}_2\text{H}_6/\text{C}_3\text{H}_8$ were investigated, it was inferred that the H atom formation mechanism is different from the OH producing one and that simple cleavage of the

O–H bond of the R–OH reaction intermediate is the dominant channel for H atom formation.²⁴ In ref 6, a low-pressure reaction pathway, $\text{CH}_2\text{O} + \text{H} + \text{H}$, was suggested for the room-temperature $\text{O}(^1\text{D}) + \text{CH}_4$ reaction, where the “second” H atom is formed by the consecutive unimolecular dissociation of $\text{CH}_3\text{O}^\ddagger$ or $\text{CH}_2\text{OH}^\ddagger$ intermediates. The assumption that at the high reagent energy of the present experiment, H atom formation also proceeds via such a three-body mechanism would lead to rather high “nonstatistical” f'_t values (see Table 2) for a process that is likely to be at least partly statistical.

V. Summary

Using the laser photolysis/laser-induced fluorescence “pump/probe” technique, an absolute reactive cross section of $\sigma^{\text{H}} = 1.4 \pm 0.5\text{ \AA}^2$ was measured for the H atom formation channel of the $\text{O}(^1\text{D}) + \text{CH}_4$ reaction at a collision energy of 37 kJ/mol. A value of $\phi^{\text{H}} = 0.30 \pm 0.11$ was determined for the H atom product branching ratio using a Langevin model for the energy dependence of the capture cross section. Comparison of the present ϕ^{H} value with results obtained at lower collision energies suggests that the relative importance of H atom formation increases slightly with increasing collision energy. The average product translational energy determined from nascent H atom Doppler profiles measured under collision-free conditions was found to be in very good agreement with previous gas-phase reaction dynamics studies carried out at lower collision energies. The observed nonstatistical product translational energy release suggests that H atom formation proceeds via the formation of a CH_3OH reaction complex followed most probably by a simple O–H bond cleavage process.

Acknowledgment. Financial support of the European Union under Contract ISC*-CT940096 of the International Scientific Cooperation program between the University of Heidelberg and the Ben-Gurion-University of the Negev (Beer Sheva, Israel) as well as support of the Deutsche Forschungsgemeinschaft via the Sonderforschungsbereich (SFB) 359 “Reaktive Strömung, Diffusion und Transport” at the University of Heidelberg is

gratefully acknowledged. Collaboration with the group of Prof. J. P. Mittal at BARC Bombay was supported by KFA Jülich and DLR Bonn under the Indo-German bilateral agreement (Project INI-207). H.R.V. would like to thank Professor G. C. Schatz (Northwestern University) for helpful communications and Professor J. Wolfrum (Director of the Institute of Physical Chemistry, University of Heidelberg) for his continuous support and his stimulating interest in the ongoing work.

References and Notes

- (1) Wolfrum, J. In *Physical Chemistry—An Advanced Treatise*; Jost, W., Ed.; Academic Press: New York, 1975; Vol. VIB. Breckenridge, W. H. In *Reactions of Small and Transient Species*; Fontijn, A., Clyne, M. A. A., Eds.; Academic Press: New York, 1983.
- (2) (a) Crutzen, P. J. In *Physics and Chemistry of Upper Atmospheres*; McCormac, B. M., Ed.; Reidel: Dordrecht, 1973. (b) Wayne, R. P. *Chemistry of Atmospheres*, 2nd ed.; Oxford University Press: Oxford, 1994.
- (3) See e.g.: (a) Levine, R. D.; Bernstein, R. B. *Molecular Reaction Dynamics and Chemical Reactivity*; Oxford University Press: Oxford, 1987; (b) *Modern Gas Kinetics*; Pilling, M. J., Smith, I. W. M., Eds.; Blackwell: Oxford, 1987. (c) *Gas-Phase Chemical Reaction Systems: Experiments and Models 100 Years after Max Bodenstein*; Wolfrum, J., Volpp, H.-R., Rannacher, R., Warnatz, J., Eds.; Springer: Heidelberg, 1996.
- (4) Brasseur, G.; Solomon, S. *Aeronomy of the Middle Atmosphere*; Reidel: Boston, 1984.
- (5) Wiesenfeld, J. R. *Acc. Chem. Res.* **1982**, *15*, 110.
- (6) Hack, W.; Thiesemann, H. *J. Phys. Chem.* **1995**, *99*, 17364.
- (7) See e.g.: Warnatz, J.; Maas, U.; Dibble, R. W. *Combustion: Physical and Chemical Fundamentals, Modeling and Simulation, Experiments, Pollutant Formation*; Springer: Heidelberg, 1996 and references therein.
- (8) Harding, L. B.; Schlegel, H. B.; Krishnan, R.; Pople, J. *J. Phys. Chem.* **1980**, *84*, 3394. Walch, S. P. *J. Chem. Phys.* **1993**, *98*, 3163.
- (9) Dombrowsky, Ch.; Hoffmann, A.; Klatt, M.; Wagner, H. Gg. *Ber. Bunsen-Ges. Phys. Chem.* **1991**, *95*, 1685 and references therein.
- (10) (a) Schmiedl, R.; Meier, U.; Welge, K. H. *Chem. Phys. Lett.* **1981**, *81*, 495. (b) Satyapal, S.; Park, J.; Bersohn, R. *J. Chem. Phys.* **1989**, *91*, 6873. (c) Wen, Y.; Segall, J.; Dulligan, M.; Wittig, C. *J. Chem. Phys.* **1994**, *101*, 5665.
- (11) Atkinson, R.; Baulch, D. L.; Cox, R. A.; Hampson, R. F. Jr.; Kerr, J. A.; Troe, J. *J. Phys. Chem. Ref. Data* **1992**, *21*, 1125 and references therein.
- (12) Davidson, J. A.; Schiff, H. I.; Streit, G. E.; McAfee, J. R.; Howard, C. J. *J. Chem. Phys.* **1977**, *67*, 5021.
- (13) Luntz, A. C. *J. Chem. Phys.* **1980**, *73*, 1143. Aker, P. M.; O'Brian, J. J. A.; Sloan, J. J. *Ibid.* **1986**, *84*, 745. Cheskis, S. G.; Iogansen, A. A.; Kulakov, P. V.; Razuvaev, I. Y.; Sarkasikov, O. M.; Titov, A. A. *Chem. Phys. Lett.* **1989**, *155*, 37. Park, C. R.; Wiesenfeld, J. R. *J. Chem. Phys.* **1991**, *95*, 8166.
- (14) Suzuki, T.; Hirota, E. *J. Chem. Phys.* **1993**, *98*, 2387. Schott, R.; Schlütter, J.; Olzmann, M.; Kleinermanns, K. *J. Chem. Phys.* **1995**, *102*, 8371.
- (15) Lin, C.-L.; DeMore, W. B. *J. Phys. Chem.* **1972**, *77*, 863.
- (16) van Zee, R. D.; Stephenson, J. C. *J. Chem. Phys.* **1995**, *102*, 6946.
- (17) Tsang, W. *Int. J. Chem. Kinet.* **1976**, *8*, 193.
- (18) Olzmann, M. *Ber. Bunsen-Ges. Phys. Chem.* **1997**, *101*, 533.
- (19) Quack, M.; Troe, J. *Ber. Bunsen-Ges. Phys. Chem.* **1974**, *78*, 240.
- (20) Brouard, M.; Duxon, S. P.; Simons, J. P. *Isr. J. Chem.* **1994**, *34*, 67.
- (21) Quoted in ref 16 as private communication from J. P. Simons.
- (22) Casavecchia, P.; Buss, R. J.; Sibener, S. J.; Lee, Y. T. *J. Chem. Phys.* **1980**, *73*, 6351.
- (23) Satyapal, S.; Park, J.; Bersohn, R. *J. Chem. Phys.* **1989**, *91*, 6873.
- (24) Matsumi, Y.; Tonokura, K.; Inagaki, Y.; Kawasaki, M. *J. Phys. Chem.* **1993**, *97*, 6816.
- (25) (a) Felder, P.; Haas, B.-M.; Huber, J. R. *Chem. Phys. Lett.* **1991**, *186*, 177. (b) Sprinsteen, L. L.; Satyapal, S.; Matsumi, Y.; Dobeck, L. M.; Houston, P. L. *J. Phys. Chem.* **1993**, *97*, 7239.
- (26) Shafer, N.; Tonokura, K.; Matsumi, Y.; Tasaki, S.; Kawasaki, M. *J. Chem. Phys.* **1991**, *95*, 6218. Hanisco, T. F.; Kummel, A. C. *J. Phys. Chem.* **1993**, *97*, 7242. Chandler, D. W. In *Combustion Research Facility News*; Sandia National Laboratories: Livermore, CA, 1997; Vol 19, No. 3.
- (27) (a) Koppe, S.; Laurent, T.; Naik, P. D.; Volpp, H.-R.; Wolfrum, J.; Arusi-Parpar, T.; Bar, I.; Rosenwaks, S. *Chem. Phys. Lett.* **1993**, *214*, 546. (b) Laurent, T.; Naik, P. D.; Volpp, H.-R.; Wolfrum, J.; Arusi-Parpar, T.; Bar, I.; Rosenwaks, S. *Ibid.* **1995**, *236*, 343.
- (28) Hilber, G.; Lago, A.; Wallenstein, R. *J. Opt. Soc. Am. B* **1987**, *4*, 1753.
- (29) Brownsword, R. A.; Hillenkamp, M.; Laurent, T.; Vatsa, R. K.; Volpp, H.-R.; Wolfrum, J. *Chem. Phys. Lett.* **1997**, *266*, 259.
- (30) Mo, Y.; Tonkua, K.; Masum, Y.; Kawasaki, M.; Sato, T.; Arikawa, T.; Reilly, P. T. A.; Xie, Y.; Yag, Y.; Huang, Y.; Gordon, R. J. *J. Chem. Phys.* **1992**, *97*, 4815.
- (31) Selweyn, G. S.; Johnston, H. S. *J. Chem. Phys.* **1981**, *74*, 3791.
- (32) Rundel, R. D. *Photochem. Photobiol.* **1983**, *38*, 569.
- (33) Matsumi, Y.; Tonokura, K.; Kawasaki, M.; Kim, H. L. *J. Chem. Phys.* **1992**, *96*, 10622.
- (34) Dóbe, S.; Bérces, T.; Temps, F.; Wagner, H. Gg.; Ziemer, H. J. *Phys. Chem.* **1994**, *98*, 9792.
- (35) Arai, H.; Kato, S.; Koda, S. *J. Phys. Chem.* **1994**, *98*, 12.
- (36) Baer, T.; DePristo, A. E.; Hermans, J. J. *J. Chem. Phys.* **1982**, *76*, 5917.
- (37) (a) Levine, R. D.; Kinsey, J. L. In *Atom-Molecule Collision Theory—A Guide for the Experimentalist*; Bernstein, R. B., Ed.; Plenum Press: New York, 1979. (b) Muckermann, J. T. *J. Phys. Chem.* **1989**, *93*, 180.